

Limits on dark matter proton scattering from neutrino telescopes using micrOMEGAs

G. Bélanger^{1*}, J. Da Silva^{2†}, T. Perrillat-Bottonet^{1‡}, A. Pukhov^{3§},

¹ *LAPTH, Université Savoie Mont Blanc, CNRS,
B.P.110, F-74941 Annecy-le-Vieux Cedex, France*

² *Consortium for Fundamental Physics, School of Physics and Astronomy,
University of Manchester, Manchester, M13 9PL, United Kingdom*

³ *Skobeltsyn Institute of Nuclear Physics, Moscow State University,
Moscow 119992, Russia*

Abstract

Limits on dark matter spin dependent elastic scattering cross section on protons derived from IceCube data are obtained for different dark matter annihilation channels using micrOMEGAs. The uncertainty on the derived limits, estimated by using different neutrino spectra, can reach a factor two. For all dark matter annihilation channels except for quarks, the limits on the spin dependent cross section are more stringent than those obtained in direct detection experiments. The new functions that allow to derive those limits are described.

*Email: belanger@lapth.cnrs.fr

†Email: dasilva@lapth.cnrs.fr

‡Email: thomas.perrillat-bottonet@polytechnique.edu

§Email: pukhov@lapth.cnrs.fr

Contents

1	Introduction	1
2	Neutrino Flux	2
3	Limits on the number of signal events	3
4	Extracting limits on DM – proton spin dependent cross sections	7
4.1	Comparison with DarkSUSY	8
4.2	Model independent limits on DM – proton cross section	10
5	Constraints on DM models	12
5.1	Z-portal dark matter	12
5.2	UMSSM	14
6	Conclusion	15
7	Acknowledgements	16
	Appendices	16
A	micrOMEGAs functions for neutrino telescopes	16
B	Examples	18
C	DarkSUSY	19

1 Introduction

The strong astrophysical and cosmological evidence for dark matter (DM) motivates numerous direct and indirect searches for DM both in astroparticle experiments and at colliders. Exploiting eventual signals from different sources could shed light on the true nature of DM. Indirect searches for DM annihilation in the galaxy are actively pursued using either positrons or antiprotons [1], photons [2] and neutrinos [3, 4]. The best limit on galactic neutrinos have been achieved by IceCube [4], however the limit on the DM annihilation cross section are still orders of magnitudes above the canonical cross section required to achieve the relic density assuming a standard cosmological scenario. Neutrino telescopes such as Super-Kamiokande [5], Baksan [6], Amanda and IceCube [7] can also observe neutrinos originating from annihilation of dark matter captured in the Sun. In that case, the neutrino flux is determined by the cross section for DM scattering on nuclei which drives the capture rate and is thus related to direct detection searches. Neutrino telescopes are sensitive to both DM nuclei spin dependent (SD) and spin independent (SI) interactions. However SI interactions are currently strongly constrained by direct detection experiments such as LUX [8] and XENON [9] whereas there is much more freedom for the SD case [10]. Moreover the coherent enhancement of SI interactions only occurs for heavier nuclei which are subdominant in the Sun. The prospects to constrain the parameter space of DM models such as the minimal supersymmetric standard model

(MSSM) using the neutrino flux from DM capture in the Sun with IceCube was examined in [11]. Furthermore limits on the spin dependent cross section based on IceCube79 results have been compared to those obtained at the LHC from monojet searches within the framework of effective field theory for a choice of DM – quark effective operators [12], neutrino telescopes were shown to be more sensitive than colliders for heavy DM masses.

In this article we present new features of `micrOMEGAs` [13–15] that allow to derive the bounds on spin dependent interactions of DM with protons using the data from IceCube22, and to obtain a likelihood that allows to combine these results with those from other searches when scanning over the parameter space of a generic DM model. We derive the bounds on spin dependent interactions with protons for any DM annihilation channel in standard model (SM) particles and compare these results with those obtained by the IceCube collaboration in two specific channels. We use the publicly available data of IceCube22, which gives a limit better than expected from statistics only because of a deficit in the number of observed events at small angles. For DM masses above 250 GeV, the limits thus obtained are expected to be comparable to those that can be reached using the newer data from IceCube79 [16]. However for lighter DM, the lower energy threshold of IceCube and DeepCore leads to a higher sensitivity than IceCube22. In the case where DM annihilates into quarks, we compare our results with those derived from monojet searches at the LHC and interpreted within an effective field theory approach assuming the same spin dependent effective operator used for DM capture. We furthermore examine the impact of IceCube22 data on the parameter space of dark matter models, for this we use a simple Z-portal model as well as U(1) extensions of the MSSM.

This article is organized as follows. Section 2 summarizes the equations used for computing the neutrino flux, section 3 describes the statistical analysis used to extract a limit. Section 4 presents the results for the upper limit on the spin dependent cross section for each individual channel. Section 5 shows the impact of IceCube results on the parameter space of two sample dark matter models. Our conclusions are summarized in section 6. The `micrOMEGAs` functions are described in the appendix as well as the method used to compare our results with `DarkSUSY` [17].

2 Neutrino Flux

After being captured, DM particles concentrate in the center of the Sun and then annihilate into Standard Model particles. These SM particles further decay producing neutrinos that can be observed at the Earth. The equation describing the evolution of the number of DM particles N_χ (assuming the DM is self-conjugate) reads

$$\dot{N}_\chi = C_\chi - A_{\chi\chi}N_\chi^2 - EN_\chi, \quad (1)$$

where $A_{\chi\chi}$ is the rate of depletion of DM,

$$A_{\chi\chi} = \frac{\langle\sigma v\rangle_{\chi\chi}}{V_{eff}}, \quad (2)$$

$\langle\sigma v\rangle_{\chi\chi}$ is the velocity averaged annihilation cross section of DM into SM particles and V_{eff} is the effective volume of DM in the Sun. E is the evaporation rate and C_χ is the capture rate of DM particles in the core of the Sun. It depends on the DM – nucleus

scattering cross section, as well as on the DM velocity distribution and local density [18]. The computation of the capture rate in `micrOMEGAs` is described in [14] and involves a contribution from spin independent and spin dependent interactions of DM on nuclei. The spin independent interactions add coherently, so the contribution of heavy nuclei is enhanced with a factor $\propto A^2$. However spin independent interactions are strongly constrained from direct detection experiments and therefore can safely be neglected as will be demonstrated in section 4. For spin dependent interactions there is no coherence effect and hydrogen gives the largest contribution, neutrino telescopes are therefore mostly sensitive to spin dependent interactions on protons.

Neglecting the evaporation rate, the solution of Eq. (1) is simply

$$\Gamma_{\chi\chi} = \frac{1}{2} A_{\chi\chi} N_{\chi}^2 = \frac{C_{\chi}}{2} \tanh^2(\sqrt{C_{\chi} A_{\chi\chi}} t) \quad (3)$$

where $t = 4.57 \times 10^9$ yrs is the age of the Sun. When the capture rate and the annihilation cross section are sufficiently large ($\sqrt{C_{\chi} A_{\chi\chi}} t \gg 1$) equilibrium is reached and the annihilation rate only depends on the capture rate, $\Gamma_{\chi\chi} = C_{\chi}/2$ and not on DM annihilation properties.

The total neutrino (antineutrino) spectrum at the Earth is proportional to the capture rate but also features a dependence on the DM annihilation channel

$$\frac{d\phi_{\nu}}{dE_{\nu}} = \frac{1}{4\pi d_{\odot}^2} \Gamma_{\chi\chi} \sum_f Br_{f\bar{f}} \frac{dN_f}{dE_{\nu}} \quad (4)$$

where $d_{\odot} = 1.5 \times 10^8$ km is the distance to the Sun, $Br_{f\bar{f}}$ the branching fraction into each particle/antiparticle final state $f\bar{f}$ and N_f are the neutrino spectra resulting from those annihilations. The neutrino spectra originating from different annihilation channels into SM particles and taking into account oscillations and Sun medium effects were computed in `WimpSim` [19], `DM ν` [20] and `PPPC4DM ν` [21]¹. We use the set of tables provided by these groups.

The distribution of the number of events in the detector, N_s , will depend on the flux of muon neutrinos. After an exposure time t_e the number of events is given by

$$\frac{dN_s}{dE} = t_e \left(\frac{d\phi_{\nu_{\mu}}}{dE} A_{\nu}(E) + \frac{d\phi_{\bar{\nu}_{\mu}}}{dE} A_{\bar{\nu}}(E) \right) \quad (5)$$

where $A_{\nu}(E)$ and $A_{\bar{\nu}}(E)$ are the effective area of the detector for neutrinos and anti-neutrinos respectively.

3 Limits on the number of signal events

To obtain the limits on the neutrino flux that could originate from DM capture in the Sun, one first needs to distinguish the signal and background events. The neutrino fluxes depend on the angle φ between the incoming neutrino and the direction of the Sun. Background events are expected to be distributed over any angle φ whereas all signal

¹Note that neutrino signals from the Sun and corresponding limits on spin dependent interaction cross sections were also investigated in [22] by focusing on the effect of internal bremsstrahlung and in [23] by paying attention on consequences of final state radiation of electroweak gauge boson.

events should occur at $\varphi = 0$. However the IceCube experiment has a finite angular resolution, the angular distribution of signal events is therefore

$$\frac{dN}{d\cos\varphi} = Ce^{\frac{\cos\varphi-1}{\sigma^2}}, \quad (6)$$

where C is a normalization constant and σ is the mean angle (in radians) [24]. The mean and median angle, φ_{med} (in degrees) are simply related through

$$\sigma = \frac{\varphi_{med}}{\sqrt{2\log(2)}} \frac{\pi}{180}. \quad (7)$$

The energy dependence of the median angle is provided on the IceCube official website². For example, for a DM of mass 1000 GeV which annihilates into W^+W^- , $\varphi_{med} = 2.9^\circ$ [25].

After estimating the background using neutrino events registered at large angles, an upper limit on the number of signal events can be obtained from the number of events registered at small angle, this method allows to get rid of systematic uncertainties. To obtain an upper limit on the number of signal events, IceCube22 uses the Feldman-Cousins method [26]. In IceCube22, 13 events were registered in the angular bin $\varphi < 3^\circ$ while 18 background events are expected. From the number of events in that angular bin we have checked that the upper limits on the total number of signal events, μ_{90} , agree with the ones presented in [25] and displayed in the second column of Table 1 for the case of DM annihilating into W^+W^- .

m_χ	μ_{90} [25]	micrOMEGAs	micrOMEGAs	DarkSUSY	IceCube22	μ_{90}^{micrO}
		PPPC4DM ν	WimpSim			
250	7.5	$1.37 \cdot 10^{-40}$	$9.51 \cdot 10^{-41}$	$8.9 \cdot 10^{-41}$	$2.8 \cdot 10^{-40}$	9.07
500	6.8	$1.48 \cdot 10^{-40}$	$1.04 \cdot 10^{-40}$	$9.7 \cdot 10^{-41}$	$3.0 \cdot 10^{-40}$	8.98
1000	6.8	$4.38 \cdot 10^{-40}$	$2.67 \cdot 10^{-40}$	$2.5 \cdot 10^{-40}$	$8.7 \cdot 10^{-40}$	8.95
3000	6.4	$3.00 \cdot 10^{-39}$	$2.06 \cdot 10^{-39}$	$2.1 \cdot 10^{-39}$	$9.9 \cdot 10^{-39}$	8.65
5000	6.8	$7.84 \cdot 10^{-39}$	$6.00 \cdot 10^{-39}$	$5.8 \cdot 10^{-39}$	$3.6 \cdot 10^{-38}$	8.67

Table 1: 90%CL upper limit on the number of signal events, μ_{90} , for DM of mass m_χ in [GeV] annihilating into W^+W^- and the corresponding limits in [cm²] on spin dependent DM – proton cross section obtained by micrOMEGAs with PPC4DM ν or WimpSim, by DarkSUSY, and by IceCube [25]. The last column contains the 90%CL upper limit on the number of signal events μ_{90} evaluated using the likelihood function of micrOMEGAs.

An alternative approach to derive the upper limit on the number of events based on Bayesian statistics has been implemented in micrOMEGAs. The likelihood function uses both information about the angular distribution and the number of digital optical modules (DOM) activated for each event. Note that the number of active DOMs is correlated with neutrino energy. The method makes use of the experimental data provided by the IceCube22 collaboration and in the DarkSUSY-5.1.2 distribution [24]³, this includes,

²<https://icecube.wisc.edu/science/data/ic22-solar-wimp>

³shared/DarkSusy/IC_data

- $A_\nu(E)$ - the effective area for neutrino detection;
- $A_{\bar{\nu}}(E)$ - the effective area for anti-neutrino detection;
- $\sigma(E)$ - the mean value of the neutrino angle resolution;
- $ch_k(N_{chan})$ - the probability to activate N_{chan} DOMs [24]. This is given for 20 energy intervals in the range $39 \text{ GeV} < E_\nu < 4 \cdot 10^5 \text{ GeV}$;
- $\frac{dN_{bg}}{d \cos \varphi}$ - the distribution of background events as a function of the angle between the incoming (anti)neutrino and the Sun;
- $ch_{bg}(N_{chan})$ - the probability to activate N_{chan} DOMs for background event;
- t_e the exposure time $t_e = 104/365 \text{ [Year]}$.

For background events, the angular and energy distribution are not expected to be correlated. Then the probability of observing a background event with an angle φ that activates N_{chan} DOMs in the detector is

$$\mathbb{P}_{bg}(\cos \varphi, N_{chan}) = \frac{dN_{bg}}{d \cos \varphi} ch_{bg}(N_{chan}). \quad (8)$$

The probability of a signal event for given neutrino ϕ_{ν_μ} and anti-neutrino $\phi_{\bar{\nu}_\mu}$ fluxes is defined as

$$\mathbb{P}_s(\cos \varphi, N_{chan}) = \sum_{k=1}^{20} \frac{n_k}{\sigma_k^2} e^{\frac{(\cos \varphi - 1)}{\sigma_k^2}} ch_k(N_{chan}) \quad (9)$$

where

$$n_k = \int_{E_{k-1}}^{E_k} \frac{dN_s}{dE} dE \quad (10)$$

$$\sigma_k^2 = \frac{1}{n_k} \int_{E_{k-1}}^{E_k} \frac{dN_s}{dE} \sigma(E)^2 dE. \quad (11)$$

The IceCube collaboration also provides the full list of events registered during the exposure time t_e , altogether 6946 events. Most of these events occur at large angle with respect to the direction of the Sun. To construct a likelihood function we avoid the regions with a large atmospheric background, and we will consider only events at angles less than φ_{cut} . The number of expected events for both background (N_{bg}) and signal (N_s) is then

$$N_{bg}^c = \sum_{N_{chan}} \int_0^{\cos \varphi_{cut}} \mathbb{P}_{bg}(\cos \varphi, N_{chan}) d \cos \varphi \quad (12)$$

$$N_s^c = \sum_{N_{chan}} \int_0^{\cos \varphi_{cut}} \mathbb{P}_s(\cos \varphi, N_{chan}) d \cos \varphi. \quad (13)$$

The likelihood function reads

$$\mathcal{L}(\alpha, \varphi_{cut}) = \frac{(N_{bg}^c + \alpha N_s^c)^{N_{tot}}}{N_{tot}!} e^{-N_{bg}^c - \alpha N_s^c} \prod_{i=1}^{N_{tot}} \mathbb{P}(\cos \varphi_i, N_{chan,i}, \alpha) \quad (14)$$

where N_{tot} is the total number of detected events for $\varphi < \varphi_{cut}$. The coefficient α varies in the range $[0, \infty]$ and

$$\mathbb{P}(\cos \varphi, N_{chan}, \alpha) = \frac{1}{N_{bg}^c + \alpha N_s^c} (\mathbb{P}_{bg}(\cos \varphi, N_{chan}) + \alpha \mathbb{P}_s(\cos \varphi, N_{chan})) . \quad (15)$$

To obtain the limit on the number of signal events we use the Bayesian approach with a flat prior distribution for the number of signal events. Then the confidence level or rather *credibility* level, is given by [27]

$$CL = \int_0^1 \mathcal{L}(\alpha) d\alpha / \int_0^\infty \mathcal{L}(\alpha) d\alpha , \quad (16)$$

Here CL represents the probability that the number of signal events is less than N_s^c .

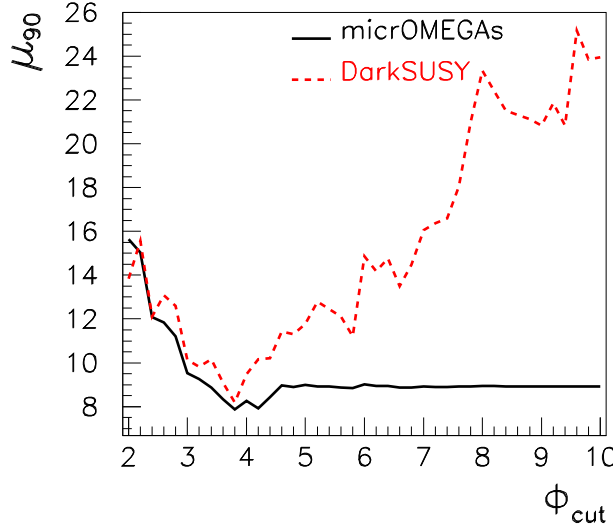


Figure 1: 90%CL limit on the total number of signal events as a function of φ_{cut} for a DM mass of 1 TeV in the W^+W^- channel obtained with **micrOMEGAs** (black) and **DarkSUSY** (dash/red).

Fig. 1 shows the dependence of the 90%CL upper limit on the number of signal events on φ_{cut} . Clearly the limit does not depend on φ_{cut} for $\varphi_{cut} > 5^\circ$, in our calculations we fix $\varphi_{cut} = 10^\circ$. For comparison the dependence on φ_{cut} of the upper limit on the number of signal events obtained with the default option in **DarkSUSY** is also displayed. Note that the two methods give similar results for $\varphi_{cut} = 3.7^\circ$, this angle also corresponds to the maximal value for $N_s^c / \sqrt{N_{bckg}^c}$. The 90%CL limits on the number of signal events calculated by **micrOMEGAs** are presented in the last column of Table 1. Despite the different statistical methods used, these numbers are in rough agreement with those extracted using only one angular bin as done by IceCube22 [25].

Note that to take into account the 20% uncertainty on the effective area, **micrOMEGAs** divides $A_\nu(E)$, $A_{\bar{\nu}}(E)$ by 1.2 when calculating the CL. Therefore we effectively rescale by

20% the limit extracted on the SD cross section and we thus obtain a more conservative limit. Note that this rescaling has no impact on the upper limit on the number of signal events.

4 Extracting limits on DM – proton spin dependent cross sections

For a given number of signal events, one can extract an upper limit on the DM – nuclei cross section, this limit will depend on the fluxes of muon neutrinos/antineutrinos that reach the detector, Eq. (4). This spectrum will depend primarily on the DM annihilation channel. When neutrinos propagate through the Sun, the spectra will be distorted by neutrino attenuation in the Sun and neutrino oscillation, furthermore other effects like electroweak bremsstrahlung can also play a role. The latter is particularly important for the electron and muon channels, otherwise these channels would not lead to neutrinos because the electron is stable and the muon is quickly absorbed in the Sun. Two sets of neutrino spectra are publicly available, **WimpSim** [19] and **PPPC4DM ν** [21]. Both spectra are implemented in **micrOMEGAs** and are used to compute the neutrino flux. We have checked the validity of our implementation by comparing with the spectra presented in [19, 21] and directly with the **WimpSim** tables implemented in DarkSUSY-5.1.2 [17]. Furthermore we have also compared our current implementation with the previous version of neutrino spectra DM ν [20] implemented in **micrOMEGAs** [14].

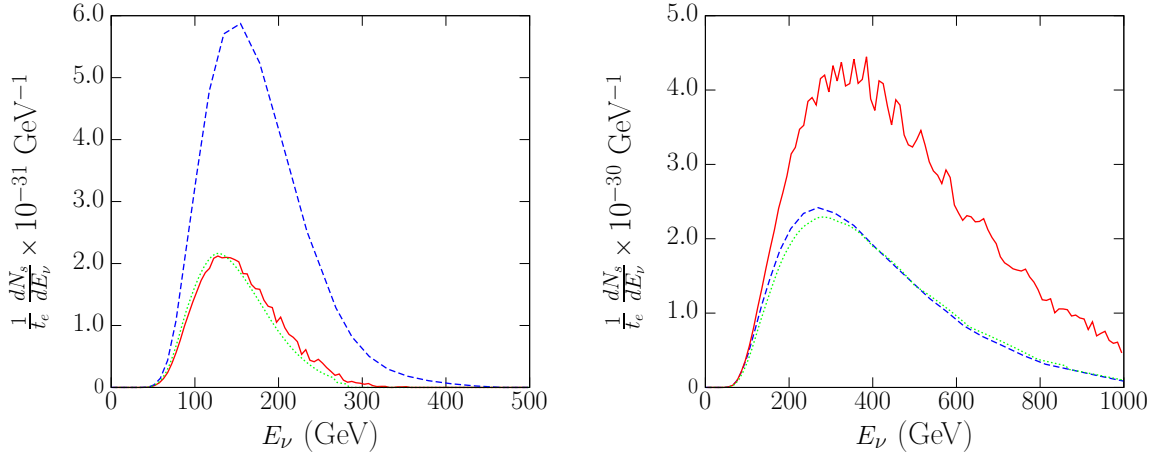


Figure 2: Comparison of neutrino spectra from **PPPC4DM ν** (dashed/blue) and **WimpSim** (full/red) for DM annihilation into $b\bar{b}$ (left) and W^+W^- (right). The DM mass is set to 500 GeV for $b\bar{b}$ and 1 TeV for W^+W^- . The spectra from the DM ν tables [20] are also displayed for comparison (dotted, light green).

For some channels the **WimpSim** and **PPPC4DM ν** spectra can be quite different, see Fig. 2 which compares the total neutrino/anti-neutrino spectra for two different channels. This difference will impact the limits derived on the DM – nucleon cross sections. The

reason for these differences is not completely clear despite the different approaches used. **WimpSim** uses Pythia [28] to get the initial neutrino spectra and a Monte Carlo approach for neutrino propagation while **PPPC4DM ν** uses GEANT [29] for the initial spectra and solves the equation for the density matrix. The discrepancy in the $b\bar{b}$ channel could be due to differences in Pythia and GEANT since the previous version of the neutrino spectrum **DM ν** [20], which relied on Pythia is in perfect agreement with **WimpSim**. We have also noted that the different treatment of the propagation in the Sun leads to different neutrino spectra even in the case where DM annihilates directly into neutrino pairs, only the **WimpSim** spectrum featuring a peak at the maximum energy. In such case it is not surprising that for all channels with an initial hard neutrino spectrum, for example W^+W^- , **WimpSim** leads to a larger and harder flux, see the right panel of Fig. 2. Another difference between the two codes is that bremsstrahlung is included in **PPPC4DM ν** , however bremsstrahlung is expected to be important mainly for light leptons.

The neutrino spectra produced by polarized vector bosons and leptons are also provided in **PPPC4DM ν** . The polarisation of vector bosons affects the spectrum of high energy neutrinos at the source, after propagation the effect is of the order of 10%. Although **micrOMEGAs** has an option to automatically compute the polarization of vector bosons in DM annihilation processes, the neutrino signal in a given model is always computed assuming unpolarized vector bosons since the effect is not large. The polarized tables can be used only in a model independent approach when one inputs a cross section and chooses explicitly the annihilation channel. On the other hand **micrOMEGAs** does not keep track of the polarization of leptons. The polarization effect can be much more important for annihilation channels into light leptons, with in particular an important contribution from left-handed light leptons (e, μ) due to bremsstrahlung. However the neutrino flux is expected to be very small for these channels as will be demonstrated in the next section. Furthermore the neutrino spectra only depend weakly on the τ polarization.

4.1 Comparison with DarkSUSY

The value of the DM – proton cross section corresponding to the upper limit on the number of signal events follows from Eqs. (3), (4) and (5). The results computed with **micrOMEGAs** and using two different choices of neutrino spectra [19], [21] are also presented in Table 1. These values are obtained starting with the upper limit on the number of events given in the first column and obtained in [25]. The results obtained with the **WimpSim** spectra are compared with those obtained with **DarkSUSY** [17] and are found to be in excellent agreement – for a description of the method used see appendix C. The limits presented by the IceCube collaboration on the spin dependent cross section are higher by roughly a factor of three [25] and are consistent with the ones obtained using the **DarkSUSY** option to compute the 90%CL using $\varphi_{cut} = 8^\circ$. Note that the limits obtained with **DarkSUSY** strongly depend on the value chosen for the angle. Since the signal is concentrated at small angle, the limits can be improved with a smaller angular cut. To first approximation, the optimal cut corresponds to the maximum of $N_{signal}(\phi_{cut})/\sqrt{N_{bg}(\phi_{cut})}$. For a 1 TeV DM annihilating into W^+W^- , the maximum is reached at $\phi_{cut} = 3.7^\circ$. For this cut, the 90% exclusion limit on the number of signal events obtained with **DarkSUSY** is 8.5, in good agreement with the **micrOMEGAs** result shown in the last column of Table 1.

In Table 2 we compare the 90% confidence limit on the DM-proton SD cross section obtained with **DarkSUSY** and with **micrOMEGAs** for the case of DM annihilation into W^+W^- .

For this we use the default “Number likelihood” flag of **DarkSUSY**, For each DM mass we find the angular cut which minimizes the ratio $N_{signal}(\phi_{cut})/\sqrt{N_{bg}(\phi_{cut})}$ where N_{signal} is the predicted number of signal events and N_{bg} is the number of background events estimated by **DarkSUSY**. Note that ϕ_{cut} does not depend on the DM-proton cross section nor on data. These results are compared with the ones obtained with **micrOMEGAs** using only angular distribution. The value obtained with **micrOMEGAs** is larger because we allow an additional 20% uncertainty to take into account the systematic error on the effective area of IceCube22. We also compare with the results obtained with **micrOMEGAs** adding the information from the energy distribution as described in the previous section. Here limits are improved noticeably for DM masses below 1 TeV, while at higher masses the two methods give similar results, this is because the energy distribution of signal and background events are similar. The same comparison is performed for the $b\bar{b}$ channel and presented in Table 3.

m_χ (GeV)	IceCube22 [25]	DarkSUSY with ϕ cut	micrOMEGAs ϕ only	micrOMEGAs $\phi + N_{chan}$	IceCube79 [16]
100		$4.19 \cdot 10^{-39}(5.6^\circ)$	$4.65 \cdot 10^{-39}$	$3.25 \cdot 10^{-39}$	$2.68 \cdot 10^{-40}$
250	$2.8 \cdot 10^{-40}$	$1.33 \cdot 10^{-40}(4.3^\circ)$	$1.56 \cdot 10^{-40}$	$1.38 \cdot 10^{-40}$	$1.34 \cdot 10^{-40}$
500	$3.0 \cdot 10^{-40}$	$1.67 \cdot 10^{-40}(3.9^\circ)$	$1.71 \cdot 10^{-40}$	$1.64 \cdot 10^{-40}$	$1.57 \cdot 10^{-40}$
1000	$8.7 \cdot 10^{-40}$	$3.12 \cdot 10^{-40}(3.7^\circ)$	$4.13 \cdot 10^{-40}$	$4.21 \cdot 10^{-40}$	$4.48 \cdot 10^{-40}$
3000	$9.9 \cdot 10^{-39}$	$2.73 \cdot 10^{-39}(3.7^\circ)$	$3.32 \cdot 10^{-39}$	$3.32 \cdot 10^{-39}$	$5.02 \cdot 10^{-39}$
5000	$3.6 \cdot 10^{-38}$	$7.24 \cdot 10^{-39}(3.7^\circ)$	$9.09 \cdot 10^{-39}$	$9.09 \cdot 10^{-39}$	$1.59 \cdot 10^{-38}$

Table 2: Comparison between limits on $\sigma_{\chi p}^{SD}$ (cm²) for $\chi\chi \rightarrow W^+W^-$ obtained by IceCube, DarSUSY for the value of ϕ_{cut} given in parenthesis and **micrOMEGAs** using only angular information (ϕ only) and also energy distributions ($\phi + N_{chan}$). All results are obtained using the **WimpSim** tables.

Finally, we comment on more recent results from the IceCube79 collaboration [16]. The lower energy threshold achievable with the use of DeepCore leads to a significant increase in sensitivity for DM masses below ≈ 250 GeV. At high masses the limits that are obtained by the collaboration in the W^+W^- and $b\bar{b}$ channel are roughly a factor 2 better than those of IceCube22 [25], see Tables 2 and 3. However we have already shown that the likelihood function implemented in **micrOMEGAs** leads also to better limits than those found in [25]. In part it is due to a statistical anomaly associated with the small number of detected events at small angles (13 events observed and 18 events expected).

Note that using the **PPPC4DM ν** spectra leads to a more conservative limit in the WW channel, this is expected considering the difference in neutrino spectra mentioned above. This is not the case in all channels as will be discussed in the next section.

m_χ (GeV)	IceCube22 [25]	DarkSUSY with ϕ cut	micrOMEGAs ϕ only	micrOMEGAs $\phi + N_{chan}$	IceCube79 [16]
100		$1.63 \cdot 10^{-36} (6.2^\circ)$	$3.74 \cdot 10^{-36}$	$2.59 \cdot 10^{-36}$	$1.47 \cdot 10^{-38}$
250		$2.94 \cdot 10^{-38} (5.0^\circ)$	$3.23 \cdot 10^{-38}$	$2.40 \cdot 10^{-38}$	$5.90 \cdot 10^{-39}$
500	$2.6 \cdot 10^{-38}$	$1.13 \cdot 10^{-38} (4.5^\circ)$	$1.13 \cdot 10^{-38}$	$9.46 \cdot 10^{-39}$	$7.56 \cdot 10^{-39}$
1000	$2.2 \cdot 10^{-38}$	$1.02 \cdot 10^{-38} (4.2^\circ)$	$1.16 \cdot 10^{-38}$	$1.05 \cdot 10^{-38}$	$1.00 \cdot 10^{-38}$
3000	$7.2 \cdot 10^{-38}$	$2.69 \cdot 10^{-38} (4.0^\circ)$	$3.55 \cdot 10^{-38}$	$3.35 \cdot 10^{-38}$	$3.16 \cdot 10^{-38}$
5000	$1.5 \cdot 10^{-37}$	$4.75 \cdot 10^{-38} (4.1^\circ)$	$7.43 \cdot 10^{-38}$	$7.28 \cdot 10^{-38}$	$7.29 \cdot 10^{-38}$

Table 3: Same as Table 2 for $\chi\chi \rightarrow b\bar{b}$.

4.2 Model independent limits on DM – proton cross section

Using the likelihood method described in section 3, we can extract the limits on spin dependent interactions of DM on protons for each channel of DM annihilation into SM particles for both the `PPPC4DM ν` and `WimpSim` spectra. The results are displayed in Fig. 3 and Fig. 4.

The strongest limits are obtained when DM annihilates into neutrinos and in particular into ν_μ or ν_τ . We find $\sigma^{SD} > 9.7 \times 10^{-42}$ pb for $m_\chi = 250$ GeV using `WimpSim`. At masses above the TeV scale the ν_τ channel becomes much more sensitive than the ν_μ channel. This is due to the fact that ν_τ can be regenerated, a charged current interaction of ν_τ with nuclei generates a τ which in turns decay rapidly into ν_τ with a high probability. On the other hand the μ generated from ν_μ by charged current interactions is stopped in the Sun medium before emitting a neutrino while the electron generated from ν_e is stable. Note that the different treatment of propagation in `WimpSim` and `PPPC4DM ν` leads to roughly a factor 2 in the 90%CL limit on $\sigma_{\chi p}^{SD}$, with the `PPPC4DM ν` leading to weaker limits because the neutrino spectrum is softer. For all masses above 60 GeV the neutrino telescope limits are more stringent than the ones from direct detection.

At high masses the second most sensitive leptonic channel is the τ channel, furthermore for all masses above 100 GeV sensitivity is better than direct detection. Note that DM annihilating into μ or electron pairs can also lead to a neutrino flux, even though muons are quickly absorbed in the Sun and electrons are stable. This is due to electroweak bremsstrahlung [21]. However the limits obtained are much weaker than for the $\tau^+\tau^-$ channel. The effect of including lepton chirality is illustrated for the $\mu^+\mu^-$ channel and basically leads to an improvement on the limit on SD cross section by a factor 2, this channel gives slightly more stringent limits than PICO in the range 600 – 1000 GeV.

The results for the W/Z and Higgs channels are displayed in Fig. 4 (left panel). The most sensitive channels are respectively ZZ and W^+W^- for DM masses below the TeV scale, while above 2 TeV the channel HH becomes slightly more sensitive. In fact at masses of 5 TeV the vector boson channels are within a factor 3 above the best leptonic channels. Using the `PPPC4DM ν` tables we have extracted independently limits from the W_T and W_L channels, the results are within 10% of those for the unpolarized case. We have also computed the limits on σ^{SD} assuming that DM annihilates solely into gluon or photon

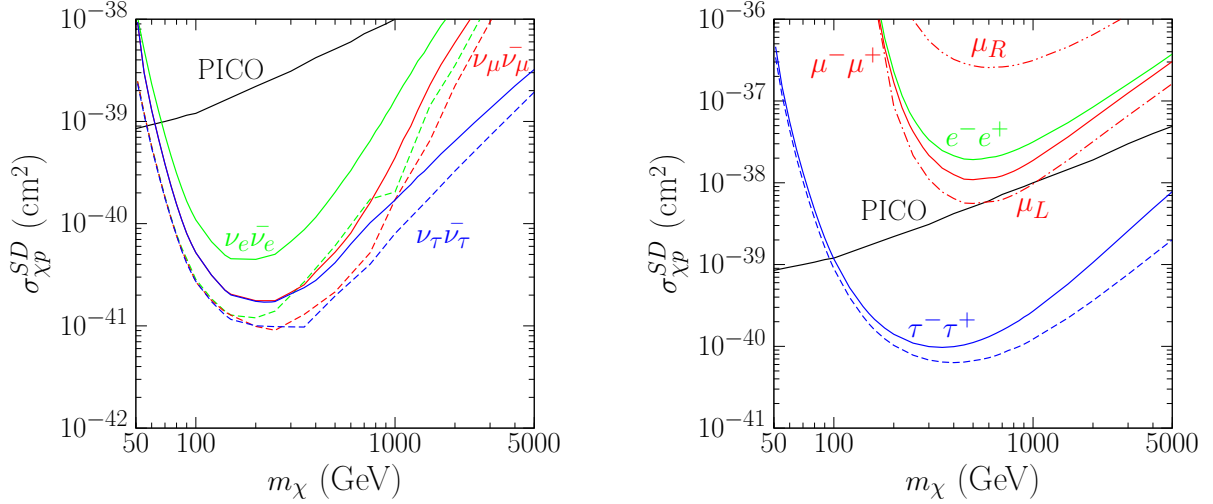


Figure 3: Upper limit on $\sigma_{\chi p}^{SD}$ for DM annihilation in $\nu_i \bar{\nu}_i$, $i = e, \mu, \tau$ (left panel) or $\tau^+ \tau^-$ (right panel) using the PPC4DM ν (full) or WimpSim (dashed) spectra. The best limit on $\sigma_{\chi p}^{SD}$ from the direct detection experiment PICO [10] is shown for comparison. The right panel also shows the limits from the light lepton channels using PPC4DM ν (full). The limits for polarized muons (dashed) are also displayed.

pairs, however they are weak. We find that for $m_\chi = 800$ GeV, $\sigma^{SD} > 6.6 \times 10^{-38}$ pb in the gluon channel and $\sigma^{SD} > 1.9 \times 10^{-38}$ pb in the photon channel. When DM annihilates into quarks the best limits are obtained for heavy quarks, in particular from the $t\bar{t}$ channel which lies about a factor of 3 above that of the ZZ case. In all those limits there is clearly a large uncertainty coming from the computation of the neutrino spectra as discussed above. Note that for light quarks it is the PPC4DM ν spectra that leads to the most stringent limits, as expected since in this case the neutrino flux is larger, see Fig. 2 for the $b\bar{b}$ channel. In fact for DM above 2 TeV, the $b\bar{b}$ channel has a comparable sensitivity (within a factor two) to the top or boson channels. For both the third generation quarks the upper limit on $\sigma_{\chi p}^{SD}$ is better than the one obtained in direct detection for masses above a few hundred GeV's. For light DM masses, these limits are however weaker than those obtained from the ATLAS and CMS collaborations in searches for DM in monojet events with 8 TeV data at the LHC [30, 31]. The collider limits presented in Fig. 4 are based on an effective field theory (EFT) approach and assume that DM couples to all quarks via the operator $1/M_*^2 \bar{\chi} \gamma^\mu \gamma^5 \chi \bar{q} \gamma_\mu \gamma^5 q$. In this approach the production of DM at colliders can be directly related to the direct detection cross sections provided the scale of new physics inducing this operator is large enough for the EFT to be valid.

We have also extracted the limits on σ^{SI} assuming DM annihilates completely in ν_τ pairs, here we assume equal cross section for scattering on protons or neutrons. We find that even with this favorable channel, neutrino telescopes cannot compete with direct

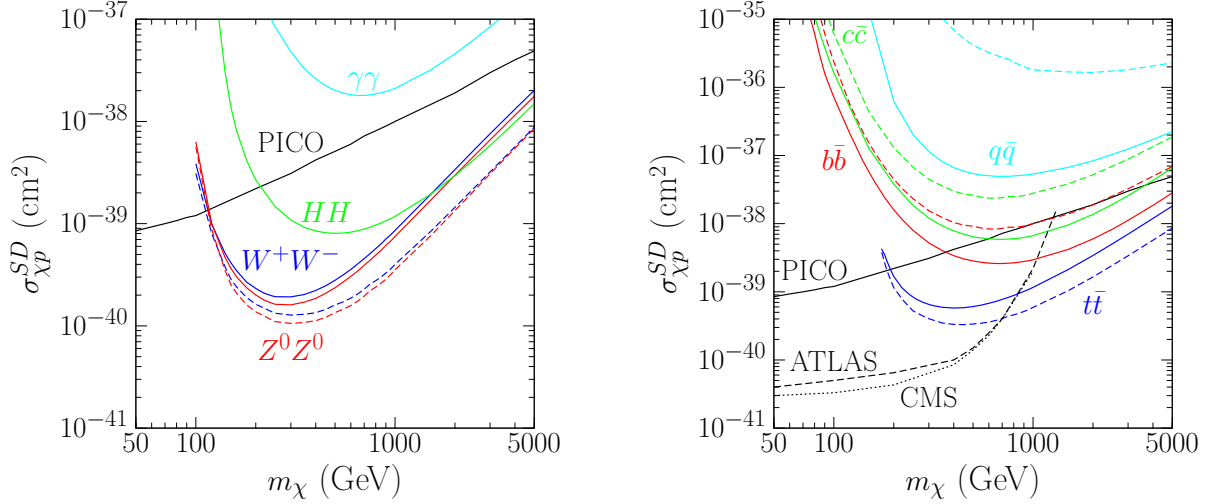


Figure 4: Upper limit on $\sigma_{\chi p}^{SD}$ for DM annihilation in W^+W^- , ZZ , HH , $\gamma\gamma$ (left panel) or $b\bar{b}$, $c\bar{c}$, $t\bar{t}$, $q\bar{q}$ (right panel) using the PPC4DM ν (full) or WimpSim (dashed) spectra. The best limit from the DM direct detection PICO [10] is also displayed as well as the limits from mono jet analysis in CMS [30] and ATLAS [31]

detection experiments, the best limit being a factor 2-10 above that of LUX [8], see Fig. 5.

5 Constraints on DM models

In a typical DM model, DM annihilation can proceed through different channels. We investigate the constraints that can be derived from IceCube data within two sample DM models, a Z-portal model [32] and U(1) extensions of the MSSM with a neutralino DM [33, 34]. Note that for this analysis, we include both SD and SI interactions and that we use the WimpSim spectra.

5.1 Z-portal dark matter

This model is a simple extension of the SM with a fermion dark matter candidate which couples to the Z with either vector (V_χ) or axial-vector couplings (A_χ), [32]. Such interaction can be obtained after symmetry breaking from the effective operator $ig/v^2 H^\dagger D_\mu H (\bar{\chi} \gamma^\mu (V_\chi + A_\chi \gamma^5) \chi)$ where H is a scalar doublet. The relevant DM interactions are described by the Lagrangian

$$\mathcal{L} = \frac{g}{4 \cos \theta_W} \bar{\chi} \gamma^\mu (V_\chi - A_\chi \gamma^5) \chi Z_\mu \left(1 + \frac{g}{m_W} H \right). \quad (17)$$

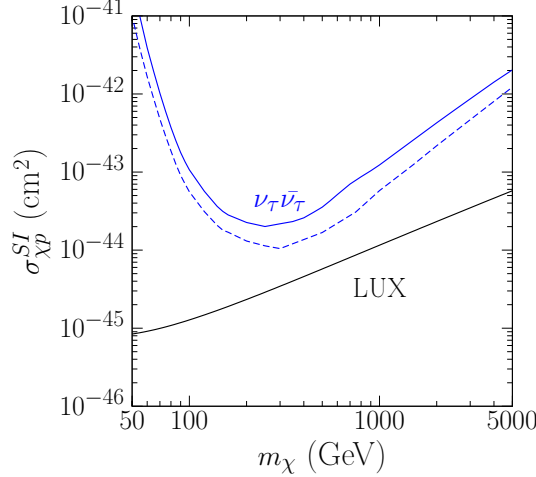


Figure 5: Upper limit on $\sigma_{\chi p}^{SI}$ for DM annihilation into $\nu_\tau \bar{\nu}_\tau$ using the PPC4DM ν (full) or WimpSim (dashed) spectra compared with the best limit from DM direct detection in LUX [8].

In addition to the DM mass the model contains only two free parameters, we choose A_χ and the ratio $\alpha = A_\chi/V_\chi$. The SD interaction which proceeds through Z exchange depends only on the axial-vector coupling (A_χ) while the SI interaction depends on the vector coupling (V_χ). When kinematically accessible, DM annihilation is mainly into W pairs, which depends on V_χ , or into final states involving ZZ, ZH and heavy fermion pairs which mostly depend on A_χ . Annihilation into leptons and light quarks is generally suppressed. Note that terms involving the Higgs in Eq. (17) are necessary to insure gauge invariance and have to be included in the relic density computation. To assess the constraints originating from IceCube22, we have performed a random scan over the free parameters of the model in the range

$$50 \text{ GeV} < m_\chi < 5000 \text{ GeV} \quad 10^{-5} < |A_\chi| < 1.0 \quad 0.1 < |\alpha| < 10^5. \quad (18)$$

We have imposed the relic density constraint from PLANCK, allowing a 10% uncertainty $0.9 < \Omega h^2/0.1199 < 1.1$ [35]. For the allowed points, we then determined those that are excluded by LUX and/or by IceCube, see Fig. 6. The former excludes points where V_χ is large while IceCube constrains points where A_χ is large. The DM mass is also relevant, for $m_{\text{DM}} < m_W$ annihilation into light quarks dominates and this region is thus poorly constrained by IceCube. In the region where $m_W < m_{\text{DM}} < m_{\text{top}}$ we find the best IceCube exclusion since annihilation into gauge bosons leads to strong exclusion. Heavier DM annihilates rather in $t\bar{t}$ or ZH , both have weaker exclusion power than the W^+W^- channel. For these masses it is generally LUX that excludes the points. After applying the PLANCK constraints, for a given dark matter mass, most points in Fig. 6

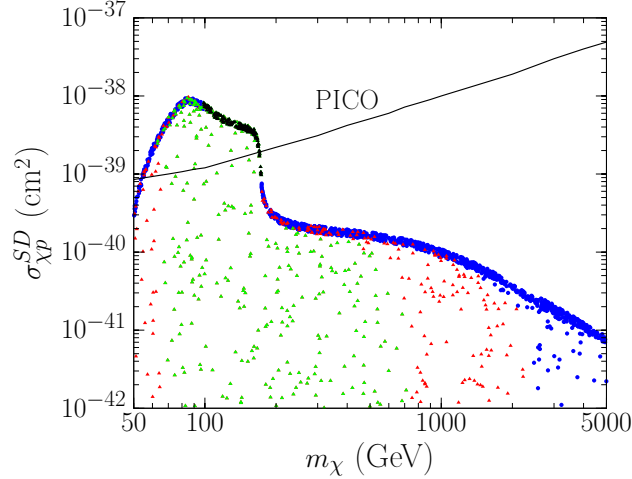


Figure 6: Constraints on the parameter space of the Z-portal model in the $\sigma_{\chi p}^{SD} - m_\chi$ plane. The color code indicates points that are constrained by IceCube22 and by LUX (green) by IceCube22 only (black) and by LUX only (red). Blue points satisfy all constraints and have a relic density in agreement with PLANCK.

are concentrated in a narrow band for the SD cross section. This is somewhat an artifact of the scan, allowing very small values of α (or a dominant V_χ coupling) would populate the region below the band. However, a large value for V_χ also leads to a large spin independent cross section, thus all those points are constrained by the LUX result even if in some case they can be also constrained by IceCube. In summary after imposing the upper limit on SI interactions, IceCube can further constrain DM in the narrow mass range 80 – 175 GeV.

5.2 UMSSM

U(1) extensions of the MSSM (UMSSM) are characterized by additional vector and scalar superfields. The model therefore features a new gauge boson (Z') and a singlet scalar, each with their supersymmetric partner, furthermore the model contains right-handed (RH) neutrinos. The lightest neutral supersymmetric particle can be the DM candidate, either a neutralino or the partner of one of the RH neutrino. Moreover new tree-level contributions to the Higgs mass make it possible to achieve a Higgs mass at 125 GeV without large corrections from the stop sector. We use the results of a random scan performed in [34] where constraints from flavor observables, the Higgs mass and couplings, and LHC searches for the Z' and for supersymmetric particles were considered. Moreover an upper bound on the relic density of dark matter was imposed [35] as well as an upper bound from direct spin independent dark matter searches from LUX [8]. We then compute

the CL for IceCube exclusion for each point of parameter space. In computing the capture rate we took into account the fact that the lightest neutralino $\tilde{\chi}_1^0$ could constitute only a fraction of the dark matter using a rescaling factor ξ defined by

$$\xi = \begin{cases} \frac{\Omega_{\tilde{\chi}_1^0} h^2}{0.1168} & \text{for } \Omega_{\tilde{\chi}_1^0} h^2 < 0.1168, \\ 1 & \text{for } \Omega_{\tilde{\chi}_1^0} h^2 \in [0.1168, 0.1208], \end{cases} \quad (19)$$

where the 2σ deviation from the central value measured by PLANCK is $\Omega h^2 = 0.1168$.

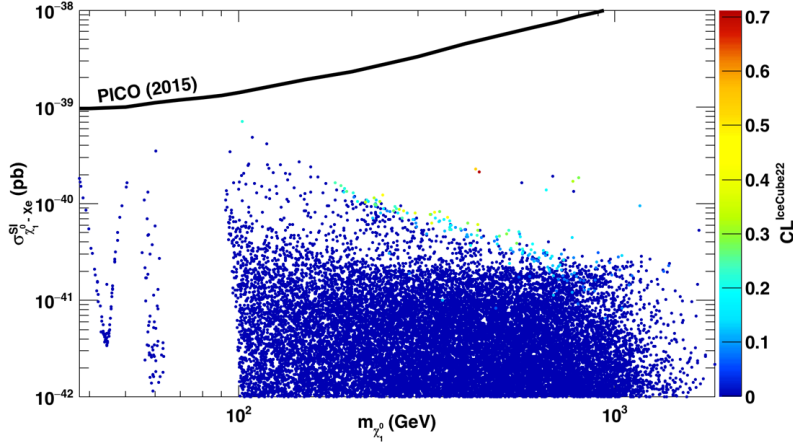


Figure 7: Allowed parameter space of the UMSSM model in the $\xi\sigma_{\tilde{\chi}_1^0-p}^{SD} - m_{\tilde{\chi}_1^0}$ plane.

Our results for all points satisfying the above mentioned constraints are shown in Fig. 7 in the spin dependent cross section vs neutralino mass plane. We did not find any point falling in the 90%CL exclusion by IceCube22, although we found such points when we ignored the LUX constraint. Moreover when assuming some regeneration mechanism for DM, which implies ignoring the rescaling of the DM local density, a few points were excluded by IceCube. Since our limits are too conservative at low masses we expect that IceCube79 data would exclude some of these points. Indeed a prospective study had shown that in the MSSM several points were excludable by IceCube+DeepCore [11]. Moreover after applying the upper limit on the SI direct detection cross section such points are concentrated at masses below 250 GeV. Although the two studies are not directly comparable since they are based on different supersymmetric models and we include most recent constraints from the LHC on the Higgs and supersymmetric sectors, it is encouraging that they qualitatively agree.

6 Conclusion

We have shown that upper limits on spin dependent interactions of DM with protons obtained from IceCube22 data are stronger than those from direct detection in a variety of channels and for a large range of masses above 100 GeV. The best limits are obtained for DM annihilation directly into neutrinos, although the $\tau^+\tau^-$, W^+W^- , ZZ channels also display good sensitivity especially for masses of a few hundred GeVs. Uncertainties from

the propagation and the oscillation of neutrinos in the Sun estimated by comparing the neutrino spectra computed by two different methods induce up to a factor two difference on the extracted limits on the DM proton spin dependent cross section. Other source of uncertainties affecting the limits derived from DM capture in the Sun arise from the DM local density, the DM velocity distribution, the escape velocity in the Sun, and the presence of a dark disc. These uncertainties were estimated to impact the capture rate by at most 50% [36]. Note however that direct detection limits are also sensitive to the uncertainties on the DM local density and velocity distribution.

A direct comparison of the LHC and neutrino telescope limits on the spin dependent cross section is straightforward in an EFT approach when we assume that DM couples to quarks only. In this case we found that the collider limits were better for light quarks and for light DM.

We have also shown that the IceCube22 results constrain some area of the parameter space of typical dark matter models, although the potential is much more limited when the current constraints on the DM spin independent scattering cross section on nucleons are taken into account first.

The results presented here and implemented in `micrOMEGAs_4.2` are based on the publicly available data from IceCube22, the `micrOMEGAs` facilities to compute limits on DM proton cross section from neutrino telescopes will be extended when more recent IceCube data becomes publicly available.

7 Acknowledgements

We thank Marco Cirelli, Joakim Edsjö and Antje Putze for useful communication. This work was supported in part by the LIA-TCAP of CNRS, by the French ANR, Project DMAstro-LHC, ANR-12-BS05-0006, by the *Investissements d'avenir*, Labex ENIGMASS and by the European Union as part of the FP7 Marie Curie Initial Training Network MCnetITN (PITN-GA-2012-315877). The work of AP was also supported by the Russian foundation for Basic Research, grant RFBR-15-52-16021-CNRS-a.

Appendices

A `micrOMEGAs` functions for neutrino telescopes

Details on all `micrOMEGAs` functions can be found in the manual contained in the `man` directory of each version. Here we present the functions to compute the (anti-)neutrino fluxes as well as the likelihood and the CL corresponding to the data of Icecube22 for DM nucleon cross sections defined in a model-independent way or within the context of a specific model.

We have introduced a new global parameter `WIMPSIM` which allows to choose the neutrino spectra. The default value `WIMPSIM=0` corresponds to the `PPPC4DM ν` [21] spectra while `WIMPSIM=1` corresponds to the `WimpSim` [19] spectra and `WIMPSIM=-1` to the `DM ν` [20] spectra implemented in previous `micrOMEGAs` versions. The parameter `forSun=1` is used to compute the signature of DM annihilation in the Sun and `Mdm` des-

ignates the mass of the DM particle.

- **basicNuSpectra(forSun,Mdm,pdg, pol, nu_spect, nuB_spect)**

calculates the ν_μ and $\bar{\nu}_\mu$ spectra corresponding to one DM annihilation into a particle-antiparticle pair with PDG code **pdg**. **Mdm** is the DM mass. Note that this routine depends implicitly on the global parameter **WIMPSIM**. The parameter **pol** selects the spectra for polarized particles available in **PPPC4DM ν** . **pol=-1(1)** corresponds to longitudinal (transverse) polarisation of vector bosons or to left-handed (right-handed) fermions, **pol=0** is used for unpolarized spectra. When polarized spectra are not available, the unpolarized ones are generated irrespective of the value of **pol**. The resulting spectrum is stored in arrays **nu_spect** and **nuB_spect**.

- **captureAux(fv,forSun,Mdm,csIp,csIn,csDp,csDn)**

calculates the number of DM particles captured per second assuming the cross sections for spin independent and spin dependent interactions with protons and neutrons **csIp**, **csIn**, **csDp**, **csDn** are given as input parameters (in [pb]). A negative value for one of the cross sections is interpreted as a destructive interference between the proton and neutron amplitudes. The first argument is the DM velocity distribution, usually we substitute **fv** = **Maxwell**. The result depends implicitly on the global parameters **rhoDM** representing the local DM density, by default **rhoDM** = 0.3 GeV/cm³.

- **IC22nuAr(E)**

effective area in [km²] as a function of the neutrino energy, $A_{\nu_\mu}(E)$.

- **IC22nuBarAr(E)**

effective area in [km²] as a function of the anti-neutrino energy, $A_{\bar{\nu}_\mu}(E)$.

- **spectrMult(Spec, func)**

allows to multiply the spectrum **Spec** by any energy dependent function **func**.

- **spectrInt(E1,E2,Spec)**

integrates a spectrum/Flux, **Spec** from E_1 to E_2 .

- **IC22BGdCos(cs)**

angular distribution of the number of background events as a function of $\cos \varphi$, $\frac{dN_{bg}}{d \cos \varphi}$.

- **IC22sigma(E)**

neutrino angular resolution in radians as a function of energy, Eq. (6).

- **exLevIC22(nu_flux, nuB_flux,&B)**

calculates the credibility level for number of signal events generated by given ν_μ and $\bar{\nu}_\mu$ fluxes, Eq. (16). The fluxes are assumed to be in [GeV km² Year]⁻¹. This function uses the **IC22BGdCos(cs)** and **IC22sigma(E)** angular distribution for background and signal as well as the event files distributed by IceCube22 with $\varphi < \varphi_{cut} = 8^\circ$. The returned parameter **B** corresponds to the Bayes factor, $\mathcal{L}(1, \varphi_{cut})/\mathcal{L}(0, \varphi_{cut})$, with \mathcal{L} defined in Eq. (14).

- **fluxFactorIC22(exLev, nu,nuBar)**

For given neutrino, **nu**, and anti-neutrino, **nuBar**, fluxes, this function returns the factor that should be applied to the fluxes to obtain a given exclusion level **exLev** in **exLevIC22**. This is used to obtain limits on the SD cross section for given annihilation channel.

- **IC22events(nu,nuB, phi, &Nsig,&Nbg,&Nobs)**

For given neutrino and anti-neutrino fluxes this routine calculates the expected number of signal **Nsig**, background **Nbg** and observed **Nobs** events. **phi** is the angular cut defined in degree units. The last parameter has to be an **int** type variable. Note that in calculating exclusion limits on cross sections, a factor 1.2 to take into account the uncertainty on the

effective area of the detector is included.

To calculate the neutrino fluxes within some theoretical DM model one can use instead of `basicNuSpectra` and `captureAux`, the function

- `neutrinoFlux(fv,forSun,nu, nu_bar)`

which calculates the muon neutrino/anti-neutrino fluxes near the surface of the Earth. This function a) calculates the capture, annihilation, and evaporation rates in Eq. (1) and b) solves it numerically; c) calculates all branchings of DM annihilation and substitute them in Eq. (4) to get the fluxes. Here `fv` is the DM velocity distribution normalized such that $\int_0^\infty v f(v) dv = 1$. The units are km/s for v and s^2/km^2 for $f(v)$. For example one can use the `Maxwell` function. The calculated fluxes are stored in the arrays `nu` and `nu_bar`, the units used are $[GeV\ km^2\ Year]^{-1}$.

In `micrOMEGAs` the neutrino spectra and fluxes are tabulated in arrays of *double* numerical type with $NZ = 250$ elements. The first (zeroth in C) element of this array contains the maximal energy of the spectrum. It usually corresponds to the DM mass, see [14]. The functions to interpolate and display spectra include

- `SpectdNdE(E,Flux)`

interpolates the tabulated spectra/flux and returns energy distribution.

- `displaySpectra(title, Emin, Emax, N, nu1,lab1,...)`

displays several spectra. Here `title` contains some text, `Emin,Emax` are the lower and upper limits, and `N` is the number of spectra to display. Each spectrum is defined with two arguments, `nu1` designates the spectrum array and `lab1` contains some text to label the spectrum.

B Examples

An example of the code that computes the 90% exclusion limits for DM-proton spin dependent cross sections for W annihilation channels and reproduces data of Tables 1, 2 and 3 reads :

```
double  nu[NZ],nuB[NZ]; // arrays for neutrino and antineutrino spectra
double  csSDp[6]={1.E-40,9.51E-41,1.04E-40, 2.67E-40,2.06e-39,6.0e-39};
                        // cross section TAB_1,4-th column
double  dSun=150E6;    // distance to Sun [km]
double  yrs=31556925.2; // year [sec]
double  Mdm[6]={100,250,500,1000,3000,5000}; // DM masses
int forSun=1;
double  exLev=0.9; // 90% exclusion confidence level
double  Nsig;      // for number of signal events

WIMPSIM=1;
printf("W channel:\n");

for(int k=0;k<6;k++)
{
    double  Crate=captureAux(Maxwell,forSun,Mdm[k],0,0,csSDp[k]*1E36,0); //DM capture rate[s]
    double  gamma=Crate*yrs/(4*M_PI*dSun*dSun)/2;
    double  f_90; // improving factor for 90% confidence level exclusion
    printf("Dark matter mass is %.2E\n",Mdm[k]);
    basicNuSpectra(forSun,Mdm[k],24/*W*/, 0, nu, nuB); // neutrino spectra
```

```

for(int i=1;i<NZ;i++) { nu[i]*=gamma; nuB[i]*=gamma;} // neutrino fluxes
if(k)
{ IC22events(nu,nuB, 10, &Nsig,NULL, NULL);
  printf("      csSDp=%.2E[cm^2] ==> Nsignal=%.2E (TAB_1 column 1)\n",csSDp[k],Nsig);
}
f_90=fluxFactorIC22( exLev,nu,nuB);
printf("      90%% exclusion limit for csSDp is %.2E[cm^2]\n",csSDp[k]*f_90);
for(int i=1;i<NZ;i++) {nu[i]*=f_90; nuB[i]*=f_90;}
IC22events(nu,nuB, 10,&Nsig,NULL,NULL);
printf("      90%% exclusion limit for number of signal events: %.2E \n",Nsig/1.2);
}

```

The code for the calculation of an exclusion level in the framework of a given model reads

```

double nu[NZ],nuB[NZ];
int forSun=1;
WIMPSIM=1;
neutrinoFlux(Maxwell,forSun,nu,nuB);
printf("IceCube22 exclusion confidence level = %.2E%%\n",100*exLevIC22(nu,nu_bar,NULL));

```

For the default data file `mssmh.par` provided in the MSSM directory of micrOMEGAs, we get a confidence level of 18%.

C DarkSUSY

DarkSUSY is generally used in the framework of some SUSY model. In order to compare the results obtained with micrOMEGAs in a model independent approach we use the following trick to calculate the number of signal events for a specific channel and a DM – nucleon cross section. The DarkSUSY subroutine `dsntICbounds` provides the number of signal events expected in IceCube22 for given annihilation channels specified by the array `wabr`, for a DM mass `wamwimp`, and for DM nucleon cross sections with the parameters `wasigsdp` for spin dependent and `wasigsip` for spin independent. We therefore redefine these parameters stored in `common /wabbranch/` before the call to the subroutine `dsntICbounds`. All cross sections should be specified in $[\text{cm}^2]$. The content of the array `wabr` is given in the file `DarkSUSY/src/wa/dswayieldone.f`. In particular `wabr(13)` corresponds to the W^+W^- annihilation channel and `wabr(25)` to the $b\bar{b}$ channel.

References

- [1] **AMS** Collaboration, L. Accardo *et al.*, “High Statistics Measurement of the Positron Fraction in Primary Cosmic Rays of 0.5500 GeV with the Alpha Magnetic Spectrometer on the International Space Station,” *Phys. Rev. Lett.* **113** (2014) 121101.
- [2] **Fermi-LAT** Collaboration, M. Ackermann *et al.*, “Searching for Dark Matter Annihilation from Milky Way Dwarf Spheroidal Galaxies with Six Years of Fermi-LAT Data,” [arXiv:1503.02641 \[astro-ph.HE\]](#).

- [3] **IceCube** Collaboration, M. Aartsen *et al.*, “The IceCube Neutrino Observatory Part IV: Searches for Dark Matter and Exotic Particles,” [arXiv:1309.7007 \[astro-ph.HE\]](#).
- [4] **IceCube** Collaboration, M. Aartsen *et al.*, “Multipole analysis of IceCube data to search for dark matter accumulated in the Galactic halo,” *Eur. Phys. J.* **C75** no. 1, (2015) 20, [arXiv:1406.6868 \[astro-ph.HE\]](#).
- [5] **Super-Kamiokande** Collaboration, T. Tanaka *et al.*, “An Indirect Search for WIMPs in the Sun using 3109.6 days of upward-going muons in Super-Kamiokande,” *Astrophys. J.* **742** (2011) 78, [arXiv:1108.3384 \[astro-ph.HE\]](#).
- [6] M. Boliev, S. Demidov, S. Mikheyev, and O. Suvorova, “Search for muon signal from dark matter annihilations in the Sun with the Baksan Underground Scintillator Telescope for 24.12 years,” *JCAP* **1309** (2013) 019, [arXiv:1301.1138 \[astro-ph.HE\]](#).
- [7] **IceCube** Collaboration, R. Abbasi *et al.*, “Multi-year search for dark matter annihilations in the Sun with the AMANDA-II and IceCube detectors,” *Phys. Rev.* **D85** (2012) 042002, [arXiv:1112.1840 \[astro-ph.HE\]](#).
- [8] **LUX** Collaboration, D. Akerib *et al.*, “First results from the LUX dark matter experiment at the Sanford Underground Research Facility,” *Phys. Rev. Lett.* **112** (2014) 091303, [arXiv:1310.8214 \[astro-ph.CO\]](#).
- [9] **XENON100** Collaboration, E. Aprile *et al.*, “Dark Matter Results from 225 Live Days of XENON100 Data,” *Phys. Rev. Lett.* **109** (2012) 181301, [arXiv:1207.5988 \[astro-ph.CO\]](#).
- [10] **PICO** Collaboration, C. Amole *et al.*, “Dark Matter Search Results from the PICO-2L C₃F₈ Bubble Chamber,” *Phys. Rev. Lett.* **114** no. 23, (2015) 231302, [arXiv:1503.00008 \[astro-ph.CO\]](#).
- [11] H. Silverwood, P. Scott, M. Danninger, C. Savage, J. Edsjö, J. Adams, A. M. Brown, and K. Hultqvist, “Sensitivity of IceCube-DeepCore to neutralino dark matter in the MSSM-25,” *JCAP* **1303** (2013) 027, [arXiv:1210.0844 \[hep-ph\]](#).
- [12] J. Blumenthal, P. Gretskev, M. Krmer, and C. Wiebusch, “Effective field theory interpretation of searches for dark matter annihilation in the Sun with the IceCube Neutrino Observatory,” *Phys. Rev.* **D91** no. 3, (2015) 035002, [arXiv:1411.5917 \[astro-ph.HE\]](#).
- [13] G. Bélanger, F. Boudjema, A. Pukhov, and A. Semenov, “MicrOMEGAs 2.0: A Program to calculate the relic density of dark matter in a generic model,” *Comput. Phys. Commun.* **176** (2007) 367–382, [arXiv:hep-ph/0607059 \[hep-ph\]](#).
- [14] G. Bélanger, F. Boudjema, A. Pukhov, and A. Semenov, “micrOMEGAs-3: A program for calculating dark matter observables,” *Comput. Phys. Commun.* **185** (2014) 960–985, [arXiv:1305.0237 \[hep-ph\]](#).

- [15] G. Bélanger, F. Boudjema, A. Pukhov, and A. Semenov, “micrOMEGAs4.1: two dark matter candidates,” *Comput. Phys. Commun.* **192** (2015) 322–329, [arXiv:1407.6129 \[hep-ph\]](#).
- [16] **IceCube** Collaboration, M. G. Aartsen *et al.*, “Search for dark matter annihilations in the Sun with the 79-string IceCube detector,” *Phys. Rev. Lett.* **110** no. 13, (2013) 131302, [arXiv:1212.4097 \[astro-ph.HE\]](#).
- [17] P. Gondolo, J. Edsjö, P. Ullio, L. Bergstrom, M. Schelke, *et al.*, “DarkSUSY: Computing supersymmetric dark matter properties numerically,” *JCAP* **0407** (2004) 008, [arXiv:astro-ph/0406204 \[astro-ph\]](#).
- [18] A. Gould, “Resonant Enhancements in WIMP Capture by the Earth,” *Astrophys. J.* **321** (1987) 571.
- [19] M. Blennow, J. Edsjö, and T. Ohlsson, “Neutrinos from WIMP annihilations using a full three-flavor Monte Carlo,” *JCAP* **0801** (2008) 021, [arXiv:0709.3898 \[hep-ph\]](#).
- [20] M. Cirelli, N. Fornengo, T. Montaruli, I. A. Sokalski, A. Strumia, and F. Vissani, “Spectra of neutrinos from dark matter annihilations,” *Nucl. Phys.* **B727** (2005) 99–138, [arXiv:hep-ph/0506298 \[hep-ph\]](#). [Erratum: Nucl. Phys.B790,338(2008)].
- [21] P. Baratella, M. Cirelli, A. Hektor, J. Pata, M. Piibeleht, *et al.*, “PPPC 4 DM ν : a Poor Particle Physicist Cookbook for Neutrinos from Dark Matter annihilations in the Sun,” *JCAP* **1403** (2014) 053, [arXiv:1312.6408 \[hep-ph\]](#).
- [22] A. Ibarra, M. Totzauer, and S. Wild, “High-energy neutrino signals from the Sun in dark matter scenarios with internal bremsstrahlung,” *JCAP* **1312** (2013) 043, [arXiv:1311.1418 \[hep-ph\]](#).
- [23] A. Ibarra, M. Totzauer, and S. Wild, “Higher order dark matter annihilations in the Sun and implications for IceCube,” *JCAP* **1404** (2014) 012, [arXiv:1402.4375 \[hep-ph\]](#).
- [24] **IceCube** Collaboration, P. Scott *et al.*, “Use of event-level neutrino telescope data in global fits for theories of new physics,” *JCAP* **1211** (2012) 057, [arXiv:1207.0810 \[hep-ph\]](#).
- [25] **IceCube** Collaboration, R. Abbasi *et al.*, “Limits on a muon flux from neutralino annihilations in the Sun with the IceCube 22-string detector,” *Phys. Rev. Lett.* **102** (2009) 201302, [arXiv:0902.2460 \[astro-ph.CO\]](#).
<https://icecube.wisc.edu/science/data/ic22-solar-wimp>.
- [26] G. J. Feldman and R. D. Cousins, “A Unified approach to the classical statistical analysis of small signals,” *Phys. Rev.* **D57** (1998) 3873–3889, [arXiv:physics/9711021 \[physics.data-an\]](#).
- [27] **Particle Data Group** Collaboration, K. A. Olive *et al.*, “Review of Particle Physics,” *Chin. Phys.* **C38** (2014) 090001.

- [28] T. Sjostrand, S. Mrenna, and P. Z. Skands, “A Brief Introduction to PYTHIA 8.1,” *Comput. Phys. Commun.* **178** (2008) 852–867, [arXiv:0710.3820 \[hep-ph\]](#).
- [29] **GEANT4** Collaboration, S. Agostinelli *et al.*, “GEANT4: A Simulation toolkit,” *Nucl. Instrum. Meth.* **A506** (2003) 250–303.
- [30] **CMS** Collaboration, V. Khachatryan *et al.*, “Search for dark matter, extra dimensions, and unparticles in monojet events in protonproton collisions at $\sqrt{s} = 8$ TeV,” *Eur. Phys. J.* **C75** no. 5, (2015) 235, [arXiv:1408.3583 \[hep-ex\]](#).
- [31] **ATLAS** Collaboration, G. Aad *et al.*, “Search for new phenomena in final states with an energetic jet and large missing transverse momentum in pp collisions at $\sqrt{s} = 8$ TeV with the ATLAS detector,” *Eur. Phys. J.* **C75** no. 7, (2015) 299, [arXiv:1502.01518 \[hep-ex\]](#).
- [32] G. Arcadi, Y. Mambrini, and F. Richard, “Z-portal dark matter,” *JCAP* **1503** (2015) 018, [arXiv:1411.2985 \[hep-ph\]](#).
- [33] J. Da Silva, *Supersymmetric Dark Matter candidates in light of constraints from collider and astroparticle observables*. PhD thesis, Annecy, LAPTH, 2013. [arXiv:1312.0257 \[hep-ph\]](#).
<https://tel.archives-ouvertes.fr/tel-00912650>.
- [34] G. Bélanger, J. Da Silva, U. Laa, and A. Pukhov, “Probing U(1) extensions of the MSSM at the LHC Run I and in dark matter searches,” [arXiv:1505.06243 \[hep-ph\]](#).
- [35] **Planck** Collaboration, P. Ade *et al.*, “Planck 2015 results. XIII. Cosmological parameters,” [arXiv:1502.01589 \[astro-ph.CO\]](#).
- [36] K. Choi, C. Rott, and Y. Itow, “Impact of the dark matter velocity distribution on capture rates in the Sun,” *JCAP* **1405** (2014) 049, [arXiv:1312.0273 \[astro-ph.HE\]](#).